

## Development of software tools for consequence assessment of aerial radioactive discharges

Petr PECHA – Radek HOFMAN, Institute of Information Theory and Automation, Academy of Sciences of the Czech Republic, Prague  
Petr KUČA, National Radiation Protection Institute, Prague  
Kateřina ZEMÁNKOVÁ, Faculty of Mathematics and Physics, Charles University, Prague

---

Deskriptory *INIS*: AIR; ALGORITHMS; DATA COVARIANCES; GAUSS FUNCTION; HYPOTHETICAL ACCIDENTS; LOCAL FALLOUT; MATHEMATICAL MODELS; METEOROLOGY; PROBABILISTIC ESTIMATION; PROBABILITY; RADIATION ACCIDENTS; RADIONUCLIDE MIGRATION; STATISTICAL MODELS

---

*The environmental system HARP is introduced. It offers an advanced interactive tool for estimation of consequences of an accident from the initial phase of radioactivity release into atmosphere and its further transport through the living environment up to human body. The system is capable to adopt the latest format of meteorological data and simulate dynamics of the releasing activity. The recent trends are followed in a risk assessment methodology insisting in transition from deterministic procedures to probabilistic approach. Special advanced statistical techniques were developed for assimilation of model predictions with data measured in terrain. The first results of the tests applied in the early and late stages of a radiation accident are promising. An illustrated example is given at the end.*

### INTRODUCTION

This article describes the most recent research achievements in the modelling of radioactivity propagation through the environment. Systematic development of the HAVAR code aimed at improving the description of uncertainty propagation through the mathematical model has resulted in the probabilistic HAVAR-RP (Reliability Predictions) version [5]. This has markedly facilitated implementation of advanced trends into the modelling, in particular, transition from the deterministic consequence assessment to the probabilistic approach. Owing to a detailed analysis of the model error covariance structure, a suitable basis has been prepared for the application of modern statistical methods for the assimilation of model predictions with real field measurements. The successor of the environmental HAVAR-RP model has been named HARP (HAzardous Radioactivity Propagation). The product offers extensive interactive software tools for input definitions of the model parameters (for release scenario definitions, dispersion and deposition submodels, dynamic

ingestion). The user-friendly output subsystem provides an interactive tool for obtaining nearly all conceivable results which are important for decision-makers (conversational mode on the “user demands” basis).

The HARP system is an outcome of the application part of the grant project supported by the Grant Agency of the Czech Republic (2007–2009), which was devised by the Institute of Information Theory and Automation, Academy of Sciences of the Czech Republic. The advanced statistical methods developed within the grant project for assimilation of model predictions for the early and late phases of a radiation accident with actual measurements are incorporated into the assimilation subsystem. The HARP system is being tuned and tested in cooperation with the National Radiation Protection Institute in Prague, where the product is online linked to the ORACLE database server and can directly input meteorological data (including short term 3-dimensional meteorological forecast). For the assimilation procedure testing purposes, the field measurements are “artificially” simulated.

## PRACTICE IN THE MODELLING OF ATMOSPHERIC DISPERSION OF POLLUTION AND ITS DEPOSITION ON THE GROUND

Models of pollution transport in the atmosphere before reaching humans constitute a significant decision-supporting tool. Various models of the propagation of radioactivity discharged into the atmosphere from a source are capable of accommodating fundamental features of the problem under different approaches. This encompasses the dimensionality, calculation domain and grid resolution, parametrization of the various physical phenomena, initial and boundary conditions, and computation-intensive techniques. It is evident that a certain compromise must be adopted between the complexity and exactness of the methodology, computer processing speed and accuracy of the results. Constraints to the capabilities of the models arise from the inherent uncertainties, limited information about the source of contamination, stochastic nature of atmospheric phenomena, limited time for generation of a reliable prediction, etc. The complexity of tracking a waste plume across the ground and its concentration depletion due to dispersion and admixture decay, washout and dryout (dry deposition) is illustrated in *fig. 1*.

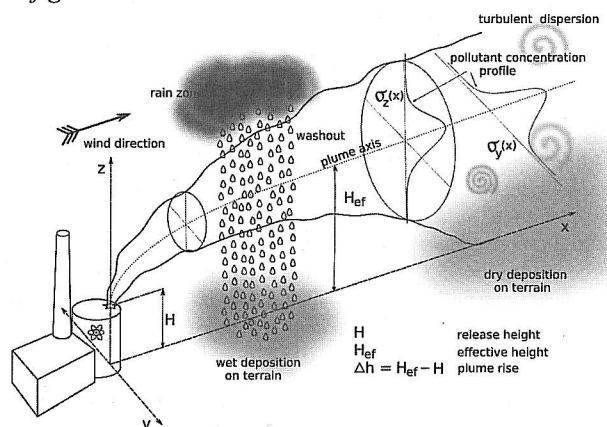


*Fig. 1. Illustration of the complex phenomena playing a role during the propagation of harmful substances discharged from a source into the atmosphere*

Various approaches to the solution of the pollution transport problem are developed in dependence on the purpose of analysis. This encompasses various domains with different scales and typical resolutions, from the microscale ( $\sim 200 \times 200 \times 100$  m; grid resolution 5 m or less) to the mesoscale ( $\sim 100 \times 100 \times 5$  km; 2 km) to the regional ( $\sim 1000 \times 1000 \times 10$  km; 20 km) continental or global scale.

The atmospheric dispersion models can be categorized with respect to their parameters regarding (i) the coordinate systems (Eulerian or Lagrangian), (ii) the wind field resolution, and (iii) the averaging procedure (respecting spatial and temporal scales of fluid-mechanical phenomena). Historically, in relation to the development of computer techniques in the 1970s, the Gaussian plume solutions

were treated. The 1980s saw the start of the development of Lagrangian puff models, as well as improvement of the three-dimensional Eulerian schemes (with few grid nodes). A major advance in the 3-D Eulerian models linked with numerical weather prediction models was achieved in the 1990s.

## THE CHOICE OF THE MODEL IS DETERMINED BY ITS APPLICATION

Several general model types are currently used: plume, segmented plume, puff, Lagrangian particle, Eulerian grid and some other special types. The classical **Gaussian approach** is still viable and successfully used in many application branches. The models have long tradition in their application to dispersion predictions for a continuous, buoyant air plume originating from a ground-level or elevated continuous source. Gaussian models can be used for non-continuous sources and changing meteorology in modification of the so-called puff approach or segmented plume scheme. Although simple, the Gaussian model is consistent with the random nature of the turbulence, it is a solution of the Fickian diffusion equation with constant  $K$  and  $u$ , and the model is tuned to experimental data and offers a rapid basic estimate with minimum computation efforts. Proven semi-empirical formulas are available for approximation of important effects, such as interaction of the plume with *near-standing buildings*, momentum and buoyant *plume rise* during release, a power-law formula for estimation of wind speed *changes with height*, *depletion* of the plume activity due to *removal processes* encompassing dry and wet deposition and radioactive decay, dependence on the *physico-chemical forms* of admixtures and the *land-use characteristics*, simplified account of an *inversion* meteorological situation and plume *penetration of inversion*, plume *lofting* above the inversion layer, account for small changes in *surface elevation*, *ground roughness* etc.

**Lagrangian** dispersion models are naturally suited to dispersion problems. Their reference system follows the prevailing atmospheric flow vector. The *Lagrangian particle dispersion* model tracks each "point-like" pollution particle on its path through the atmosphere. The particles are drifted with the mean wind velocity and are additionally subjected to random turbulences. The concentration distribution is obtained by counting particles in a given sampling volume. The *Puff Particle Model* (PPM), using the concept of relative diffusion of a puff, is an advanced effective modification for mesoscale modelling. The pollution source quantities are combined together in a puff (parcel of particles) containing a finite number of infinitesimal particles. The motion of each particle is determined by the mean fluid velocity of the puff and the turbulent sub-grid scale velocity. Lagrangian trajectories are numerically simulated for a large number of such particles, and finally the particles in given sampling volumes are counted. Since a large number of particles ( $10^4 - 10^5$ ) has to be simulated, the methods require a powerful computational tool.

Eulerian dispersion models solve the pollutant problem described by a diffusion equation in the framework of a fixed 3-D Cartesian equidistant computation grid. The pollution concentration is simulated in an array of fixed Earth-based computational cells. The method is capable of providing detailed information on the concentration distribution even if complex boundary conditions in the microscale domain are imposed. The Eulerian approach is very computationally expensive and numerical problems can sometimes arise.

The Lagrangian or Eulerian model is a suitable tool for detailed short-distance modelling and complex boundary conditions. In particular, the specific current developments are oriented on the analysis of hypothetical terrorist attacks with RDD in urban areas. The models can be nested within the Gaussian model which can describe further propagation at longer distances from the source. The primary dispersion algorithm developed specifically for the HARP system is based on a segmented Gaussian scheme [7,8]. The main objective is the development of a most rapid and accurate computer code for the purposes of not only deterministic estimation but, in particular, for multifold repetitive sequential Monte Carlo calculations (for many thousand realisations of the random model parameters). Such a code is prerequisite for a probabilistic assessment and application of advanced statistical assimilation techniques of Bayesian filtering.

## ADEQUATE AND UP-TO-DATE DATA FOR ADVANCED MODELLING

Basic prerequisites for utilization of the advanced models include availability of the latest formats of all inputs, such as geographical and demographical databases, field measurements, estimation of the source term, vegetation periods and many others. However, what is of fundamental importance for an accurate assessment of the consequences of the accident, is the incorporation of an adequate description of the atmospheric flow fields. The mathematical model should accommodate all details of the current meteorological forecasts. More informative meteorological data also make for improvement of the former classical Gaussian approach (direct evaluation of atmospheric turbulence through the friction velocity and Monin-Obukhov length)

As early as 1904, Vilhelm Bjerkens demonstrated that the evolution of the state of the atmosphere can be described by a set of seven equations with seven unknowns, viz. 3 momentum conservation equations for each wind velocity component, continuity equation, equation of state of ideal gases, energy conservation, and water vapour mass conservation. At the same time, this system of differential equations describes a chaotic nature that imposes limits on the stability of weather predictions and weather predictability at large. In a chaotic system, the errors introduced can grow with time. This poses an ultimate problem in meteorological forecasting.

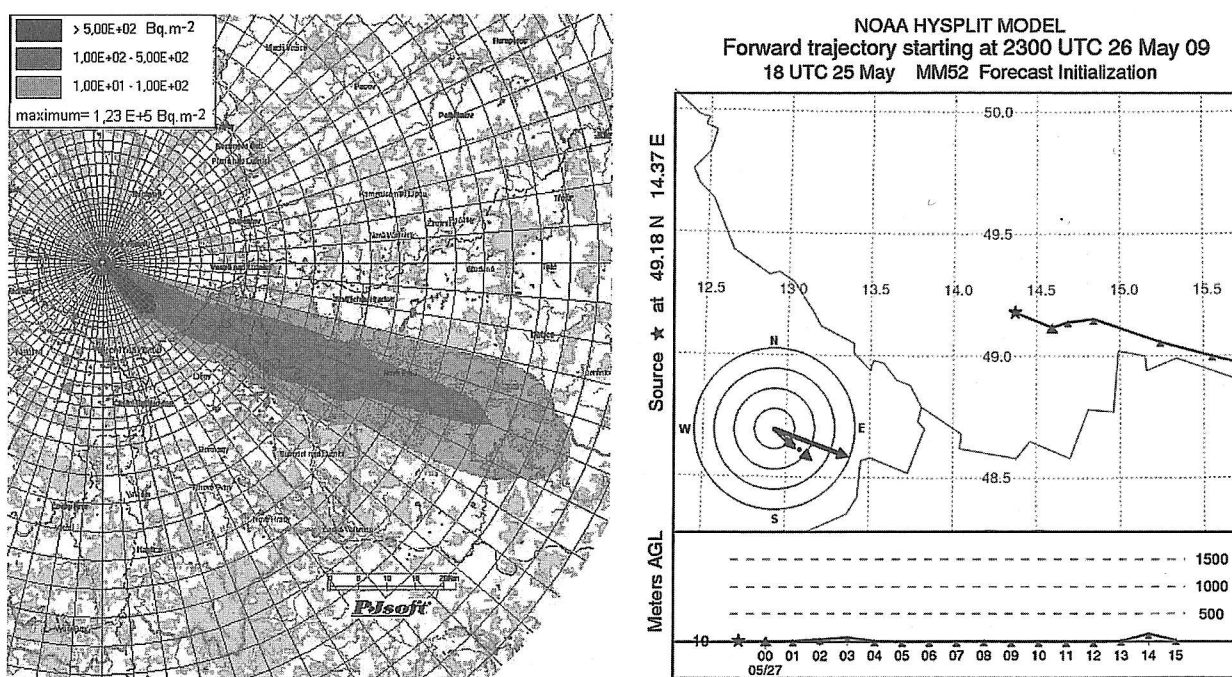


Fig. 2. Hypothetical release of  $^{131}\text{I}$  for real meteorology of May 26, 2009. Release start at 23.00 UTC, duration 1 hour; discharged activity  $6.0\text{E}+11 \text{ Bq}$ . Left: Segmented Gaussian plume model with a limited 3-D ALADIN short term forecast (trace of  $^{131}\text{I}$  deposition on the ground after 5 hours). Right: Cloud trajectory for the same situation and scenario, calculated by the HYSPLIT code [2] with 3-D meteorological forecast in the MM5 format. The wind rose in the bottom left corner represents the wind direction during the first hour: forecast from ALADIN (double line), forecast from MM5 (solid line), real measurements (dotted line).

And it is assimilation of the weather predictions with meteorological measurements that has been found to be an efficient technique in the struggle against the tendency to destruction of model knowledge.

The environmental HARP model is online connected to meteorological data provided by the Czech Hydrometeorological Institute (CHMI). For the Dukovany and Temelin nuclear power plants, both point and gridded ( $160 \times 160$  km, ALADIN format) short term (48 hours) forecast data are available. Several comparisons between SGPM and HYSPLIT [2] (HYbrid Single-Particle Lagrangian Integrated Trajectory model) results have been made within the grant project. A proper sequence of the 3-D meteorological forecast in the MM5 format input to the HYSPLIT calculations was obtained thanks to cooperation with specialists from the MEDARD project at the Institute of Computer Science, Academy of Sciences of the Czech Republic. Illustrative partial results are shown in *fig. 2*. Some distinct differences have been found between wind field predictions obtained with ALADIN and with MM5, and real data, which are available for this period. Presumably, the gridded meteorological data (provided on a  $9 \times 9$  km mesh grid) are sometimes incapable of accommodating the local changes properly. The need for an intelligent meteorological pre-processor of some kind is evident.

### SEGMENTED GAUSSIAN PLUME MODEL (SGPM) OF AERIAL TRANSPORT

Airborne admixtures are drifted by the surrounding ambiance and, precisely speaking, the equation describing the pollution transport should be solved in parallel to the equations describing the state of the atmosphere. Because of practical infeasibility, the pollution transport is analyzed separately whereas the meteorological fields are input to the calculations externally. The analytical solution of the diffusion equation can only be found under drastic simplifications and for simple initial and boundary conditions.

Our approach is based on Gaussian dispersion modelling using further modifications of a certain numerical scheme accounting for the real situation. The basic idea consists in a synchronization of the available short-term meteorological forecast provided by the Czech meteorological service with the release of dynamic of harmful substances discharged into the atmosphere. Real dynamics of the accidental release is transformed into an equivalent number  $G$  of consecutive homogeneous segments 1 hour long. The movement of each segment is driven by the short-term meteorological forecast for the corresponding hours of propagation. The shape of the segment spreading is simulated by a "Gaussian droplet" emerging from the simplified solution of the diffusion equation.

The principle of the numerical SGPM algorithm initially developed for the HARP system is illustrated in *fig. 3*. The total movement of each partial Gaussian one-hour segment during the next one-hour interval is

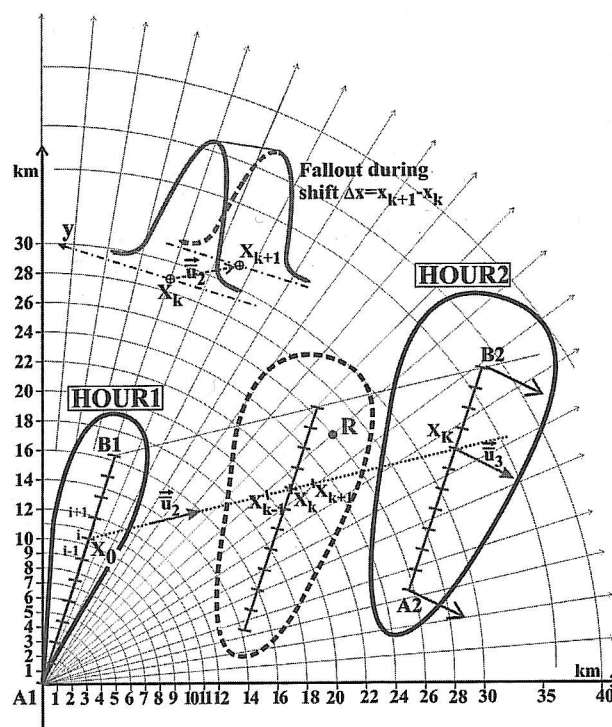


*Fig. 3. The segmented Gaussian plume approach to the modelling of pollution propagation in the atmosphere*

modelled as a sequence of partial elementary shifts  $k$  ( $k=1, \dots, K$ ;  $K=30 \div 50$ ). Let us follow the one-hour segment in its position after the 1st hour of motion. The position is designated HOUR1 in *fig. 3*. It is described by the Gaussian straight-line approximation in a 1-hour prolongation ("Gaussian droplet"). The meteorological forecast for the 2nd hour is used and the HOUR1-segment is drifted during the whole second hour as determined by the wind vector  $u_2$ , class of atmospheric stability  $class_2$  and precipitation intensity  $v_2$ . The motion of the "droplet" from position HOUR1 to HOUR2 is then modelled as a sequence of  $K$  partial shifts starting from a known initial position on the HOUR1 plume segment with axis (A1; B1) up to HOUR2 with axis (A2; B2). The near-ground activity concentration in air  $C$  ( $Bq \cdot m^{-3}$ ) of a radionuclide is calculated step by step after each elementary shift  $k$ .

SGPM uses the "source depletion" approach based on a separation of the pure dispersion solution  $C^{disper}$  and the "removal" component described by the plume depletion factors  $f_R^m, f_F^m, f_W^m$  due to radioactive decay ( $R$ ) and dry ( $F$ ) and wet ( $W$ ) deposition in dependence on the physico-chemical form of the nuclide  $n$  (henceforth the index  $n$  is omitted in this paragraph). The activity concentration decrease within the elementary droplet shift  $k \rightarrow k+1$  can be described schematically by separating the pure dispersion component  $C^{disper}$  and the depletion factors:



$$\begin{aligned}
 C(X_{k+1}) &= C^{disper}(X_{k+1}) \cdot \Delta f_R^{k \rightarrow k+1} \cdot \Delta f_F^{k \rightarrow k+1} \cdot \Delta f_W^{k \rightarrow k+1} \\
 \text{Rad. decay: } \Delta f_R^{k \rightarrow k+1} &= \exp(-\lambda |X_{k+1} - X_k| / u_2) \\
 \text{Dryout: } \Delta f_F^{k \rightarrow k+1} &= 1 - \sqrt{2/\pi} \frac{v_g \left( \overline{X^{k,k+1}} \right)}{u_2 \sigma_z \left( \overline{X^{k,k+1}} \right)} \exp \left[ \frac{H_{ef}^2}{2\sigma_z^2 \left( \overline{X^{k,k+1}} \right)} \right] \\
 \text{Washout: } \Delta f_W^{k \rightarrow k+1} &= \exp(-\Lambda |X_{k+1} - X_k| / u_2)
 \end{aligned} \tag{1}$$

The Gaussian solution for  $C^{disper}(X_{k+1})$  has been derived in [7,8]. In Eq. (1)  $\lambda$  stands for the decay constant,  $\Lambda$  is the washout coefficient, and  $H_{ef}$  is the effective plume height. The dry deposition velocity  $v_g$  and vertical dispersion coefficient  $\sigma_z$  are related to the centre of abscissa  $\overline{X^{k,k+1}}$ ,  $|X_k - X_{k+1}|$  is the distance between the points  $X_k$  and  $X_{k+1}$ .

The contribution of the segment to the TIC (Time Integral of near ground activity Concentration) in the receptor point R during its motion from partial position  $k$  to the next partial position  $k+1$  is expressed as

$$\Delta TIC(R; k) = \frac{C(R, k) + C(R, k+1)}{2} \cdot \Delta t(k) \tag{2}$$

The time difference  $\Delta t(k) = |X_k - X_{k+1}| / \bar{u}_2$  is set identical for each  $k$ . The TIC value at the receptor point R from all consecutive partial shifts  $k, k=1, \dots, K$  is given by:

$$TIC(R; K) = \sum_{k=1}^K \Delta TIC(R; k) \tag{3}$$

A similar approach can be adopted as regards activity deposition on the ground around the receptor point R. The deposited activity at the receptor point R due to the dry and wet effects during an elemental shift  $\Delta t(k)$  is approximated as:

$$\Delta DEP(R; k) = \Delta DEP^{dry} + \Delta DEP^{wet} \tag{4}$$

The contribution from the dry fallout is

$$\Delta DEP^{dry} = \Delta TIC(R; k) \cdot v_g \tag{4a}$$

The contribution from the wet deposition in the BOX model approach (full vertical homogenization along the mixing layer with height  $H_{mix}$ ) is:

$$\Delta DEP^{wet} = \Delta TIC(R; k) \cdot \Lambda \cdot H_{mix} \tag{4b}$$

The deposited activity at the receptor R at the time of shift  $k$  is the sum of deposited activities from all previous shifts  $j$  starting from position HOUR1 for  $j=1$  up to the monitoring shift  $k$ . Taking into account radioactive decay, activity deposition at the time of the shift  $k$  is given by

$$DEP(R; k) = \sum_{j=1}^k \{ \Delta DEP(R; j) \cdot \exp[-\lambda(k-j) \cdot \Delta t] \} \tag{5}$$

The deposited activity at the receptor R after the whole movement of the segment from its position HOUR1 to HOUR2, denoted  $DEP(R, K)$ , is calculated by using the previous equation after substituting  $k = K$ . Now the time integral of activity deposited during the complete motion of the plume segment from HOUR1 to HOUR2 can be calculated as

$$TID(R; K) = \sum_{k=1}^K \{ DEP(R; k) \cdot \Delta t \} \tag{6}$$

The basic SGPM model of aerial transport of radioactivity has been verified by extensive comparative analysis [5] including COSYMA and RODOS runs.

An example of SGPM calculation is given in *fig. 4* for the following fictive imaginary scenario: release of  $^{131}\text{I}$  from the Dukovany NPP; release started at 17.00 CET on June 25, 2008 (summer storm with rather rapid meteorological changes). The release is assumed to last 1 hour, total  $^{131}\text{I}$  activity released into the atmosphere  $7.48\text{E}+13$  [Bq], release height 45 m, dispersion calculated for a smooth European type ground (SCK/CEN formulae). Two kinds of short-term meteorological forecast are generated and transmitted from the CHMI to the ORACLE database:

**Scheme 2:** Simple short-term meteorological forecast for a single NPP reference point. Each hourly segment of release is driven by hourly meteorological conditions, which change in time (each hour) but are applied in the whole region in the same way at once (*time dependent, spatially constant*).

**Scheme 3:** Gridded 2-D and 3-D meteorological data on a mesoscale region  $160 \times 160$  km around each NPP. Each hourly segment of release is driven by hourly meteorological conditions that are changing in time (each hour) and space (*time dependent, spatially dependent*).

The SGPM algorithm can accommodate both schemes. The scheme in *fig. 4* subjects the "Gaussian droplet" to translation, rotation and squeezing during its transport within the successive 1-hour meteorological phases. A more accurate determination of the affected areas can be expected if a more precise (scheme 3 gridded data) meteorological forecast is used [8].

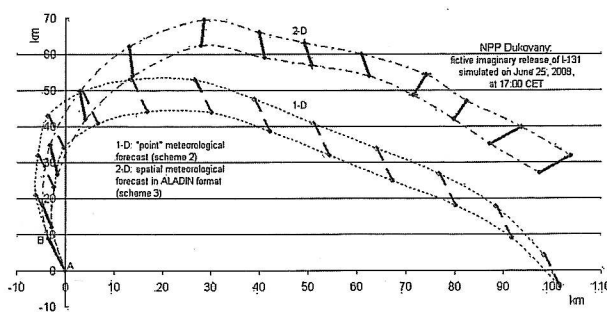


Fig. 4. Abscissa AB illustrates the trace of the  $^{131}\text{I}$  plume during the first hour of release. Its stepwise movement in the next hours is modelled by using a 1-D meteorological forecast (Scheme 2) and by using more realistic spatial 2-D forecast (Scheme 3) in the ALADIN format. The significance of using the more precise Scheme 3 data is evident.

### GENERAL SCHEME FOR THE COMPOSITION OF THE OUTPUT RADIOLOGICAL QUANTITIES

As mentioned above, the hypothetical radioactivity release is equivalently segmented into hourly segments  $g$ ,  $g \in \{1, 2, \dots, G\}$ . Each segment  $g$  is modelled in its subsequent meteorological phases  $f$ ,  $f \in \{1, 2, \dots, NFAZ(g)\}$  taking into account the hourly meteorological forecast.  $NFAZ(g)$  is the total number of consecutive hours of the segment  $g$  tracking. The hourly plume segment  $g$  in its hourly meteorological phase  $f$  is denoted  $\text{puf}\{g; f\}$ . The final total value of a certain significant output  $\gamma$  at the receptor point  $R$  belonging to the effect of nuclide  $n$  is given by superposition of the results for all plume segments in all their meteorological phases according to the scheme

$${}^n\gamma_{TOTAL}(R) = \sum_{g=1}^G \left\{ \sum_{f=g}^{NFAZ(g)} {}^n\gamma_{\{g;f\}} \right\} \quad (7)$$

A fundamental role among the simulated output categories is played by the four main nuclide dependent variables  $\gamma$  related to the early phase of the accident. Specifically, the various  $\gamma$  values can represent:

- near-ground activity concentration in air – spatial distribution around the source in the polar nodes [ $\text{Bq}\cdot\text{m}^{-3}$ ],
- time integral of the near-ground activity concentration in air – spatial distribution [ $\text{Bq}\cdot\text{s}\cdot\text{m}^{-3}$ ],
- activity deposited on the ground – spatial distribution [ $\text{Bq}\cdot\text{m}^{-2}$ ],
- time integral of activity deposited on the ground – spatial distribution [ $\text{Bq}\cdot\text{s}\cdot\text{m}^{-2}$ ].

All the other possible outputs  $\gamma$ , such as 2-D distributions of irradiation doses both in the early and late stages of the accident, countermeasure estimation, long-term evolution of specific radioactivity levels in agricultural products and food-ban effectiveness assessment, long-term doses from resuspension, etc., can be calculated directly from those four driving quantities applying additional time integration. For example, the dose estimates  $\Psi$  (related to the age category  $a$ ) can be schematically described as:

$$\Psi_{TOTAL}(R; a; T) \approx \sum_{n=1}^{NU} [{}^n\gamma_{TOTAL}(R) \cdot I(T) \cdot {}^n\Omega^{conv}(a)] \quad (8)$$

where  $\Omega$  encompasses relevant conversion factors. Time integration of the long-lasting effects (e.g. radioactive decay, activity migration in soil) up to time  $T$  is formally denoted  $I(T)$ . It can largely be expressed analytically. Somewhat complicated is the computation of the time-integrated activity intakes by using the dynamic model of ingestion developed specifically for the HARP system.

### A FLEETING GLANCE AT THE PROBABILISTIC APPROACH

So far, we examined the simulation SGPM model under an implicit assumption of the best estimated (expected) values of the model parameters. It represents a simplified conceptual view of reality where the inherent uncertain features of nature are incorrectly neglected. Uncertainties of the model parameters are due to imperfections in both the conceptual model (algorithm limitations, simplifications during parametrization, stochastic nature of some submodel parameters, input data measurement errors) and the computational scheme (computation grid step, averaging land-use characteristics, averaging times for dispersion parameters, etc.).

First, let us highlight the difference between the variability and uncertainty of a variable. Variability reflects changes in a quantity over time, over space or across individuals in a population. Variability reflects diversity or heterogeneity in a well-described population. The term “uncertainty” incorporates stochastic uncertainties, structural uncertainties due to partial ignorance or incomplete knowledge associated with lack of perfect information about poorly described phenomena or models and input model uncertainties. The HARP system respects the variability concept wherever possible. The quantity with a variability character is not treated as a single variable: instead, it is split into a set of particular variables entering the calculations individually. As an example, mention the calculation of doses where, rather than one single quantity related to all population age categories (comprising a certain effect of inter-categorical variability) we generate a set of values, each relating to a specific age category. Discriminating between the notions of variability and uncertainty is crucial for meteorological inputs as well. Seasonal and diurnal changes are the cause of meteorological data variability whereas fluctuations about nominal (forecast) values for the particular meteorological situation related to the specific time of release is regarded as uncertainty.

Now, return to the uncertainty treatment. In the following text, capital symbols are related to the random variable whereas lower case symbols stand for concrete values selected from the corresponding random distribution. Let  $\Theta \equiv [\Theta_1, \Theta_2, \dots, \Theta_M]^{-1}$  denote a vector of  $M$  random model parameters  $\Theta_m$  with a corresponding sequence of random distributions  $D_1, D_2, \dots, D_M$  which are usually

selected on the basis of consensus among experts (range, type of distribution, potential mutual dependencies). The model parameters usually have a physical meaning, such as the amount of radioactivity discharged, atmospheric dispersion parameters, uncertainties related to the dry and wet radioactivity fallout, wind field components, and the like. Expression (7) should be valid for all nodes  $R_i$ ,  $i \in \{1, \dots, N\}$  of the polar computational grid. For example for the 2-D spatial distribution of activity deposited on the ground we have  $N=2800$  for 35 radial distances and 80 angular sectors. Thus, Eq. (7) can be considered in a vector form,  $\gamma$  being a vector of dimension  $N$  with components  $\gamma_i = {}^n\gamma_{TOTAL}(R_i)$ . Having on mind the random character of the model parameters, Eq. (7) can be converted to:

$$\Gamma = \mathfrak{R}^{SGPM}(\Theta) \quad (9)$$

where operator  $\mathfrak{R}^{SGPM}$  represents the numerical SGPM algorithm outlined in (7).  $\Gamma \equiv [\Gamma_1, \Gamma_2, \dots, \Gamma_N]^{-1}$  is a vector of the output variable  $\gamma$  with random components  $\Gamma_i$ . The unobservable random vector  $\Gamma$  is introduced into the assimilation notation as a state vector. The bold symbol  $\gamma$  stands for a vector of particular realizations of  $\Gamma$ . From a physical perspective, we can look at Eq. (9) as a random "trajectory" of the resulting variable of interest ( $\gamma$  can stand e.g. for the 2-D trajectory of the trace of activity deposited on the ground, 3-D for the activity concentration in the air, etc.). Analogously, vector  $\gamma$  can be perceived as a particular trajectory (given in discrete points). The sampling-based method consists in the calculation of the  $k$ -th concrete realization  $\gamma^k$  of the state vector  $\Gamma$ , repeatedly in two steps:

1) Generation of a particular  $k$ -th sample of the parameter vector:

$$\Theta^k \equiv [\theta_1^k, \dots, \theta_m^k, \dots, \theta_M^k]^{-1} \quad (10)$$

where  $\theta_m^k$  is the  $k$ -th realisation of the  $m^{th}$  random parameter  $\Theta_m$ .

2) Propagation of the sample  $k$  through the model, it means the calculation of the corresponding resulting  $k$ -th realisation of the trajectory as:

$$\gamma^k = \mathfrak{R}^{SGPM}(\theta_1^k, \dots, \theta_m^k, \dots, \theta_M^k) \quad (11)$$

where  $\gamma^k$  is the  $k$ -th trajectory realization, which is a vector with components  $\gamma_i^k$ ,  $i \in \{1, \dots, N\}$ .

The adopted Monte Carlo modelling scheme uses the LHS (Latin Hypercube Sampling) stratified sampling procedure. The HARP code comprises an interactive subsystem for generating  $K$  LHS samples for various types of random distribution  $D_m$  of the parameter vector  $\Theta \equiv [\Theta_1, \dots, \Theta_m, \dots, \Theta_M]^{-1}$ . A technique for correlation control between components  $\Theta_m$  is included. The resultant mapping of pairs of vectors is given by

$$[\gamma^k; \theta^k]_{k=1, \dots, K} \quad (12)$$

As described above, the trajectory  $\gamma^k$  represents an  $N$ -dimensional vector of the values of quantity of interest  $\gamma$  in  $N$  spatial nodes. Provided that the value of  $K$  is sufficiently high (several thousands), Eq. (12) represents the key scheme for uncertainty analysis and sensitivity studies. Statistical

processing of the pairs (12) can provide the extent of uncertainty on the predicted consequences and yields various statistics, such as the sample mean and variance, percentiles of the uncertainty distribution on the specific quantity, uncertainty factors, reference uncertainty coefficients, etc. Simulation of uncertainty propagation through the model is of cardinal importance for the introduction of advanced methods into the modelling, since it provides:

- essential data for the transition from the deterministic consequence assessment procedure to the probabilistic approach which enables more informative probabilistic answers on the assessment questions to be generated,
- detailed analysis of the model error covariance structure, thus making it possible to improve the model prediction reliability based on the application of advanced statistical techniques of assimilation of mathematical prognoses to real measurements incoming from the field.

An example of one of the many possible modes of the probabilistic estimation is illustrated in *fig. 5* for the case of hypothetical release of  $^{137}\text{Cs}$ . The release scenario with the local atmospheric precipitation, which occurred between Hours 5 to 6 after the beginning of the release (random rain intensity has uniform distribution  $U[0; 6\text{mm/h}^{-1}]$ ), is described in [6].

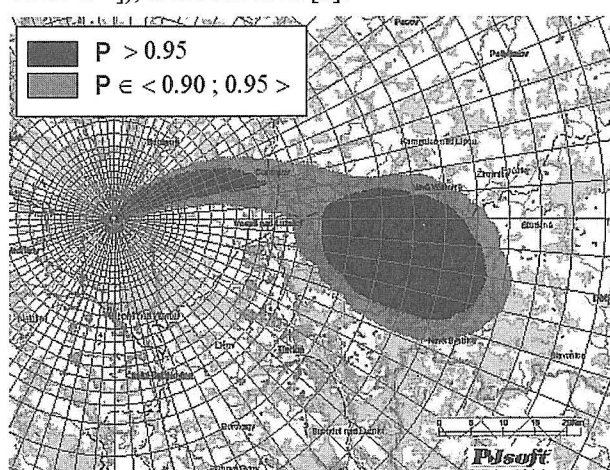


*Fig. 5. Isolines of probability  $P(\text{depo} > D^{\text{lim}})$  that the chosen  $^{137}\text{Cs}$  deposition limit  $D^{\text{lim}} = 1000 \text{ Bq/m}^2$  will be exceeded. The probabilistic SGPM analysis includes 5000 random samples. The retrospective meteorological forecast sequence from June 28, 2002 with release start at 00 UTM was used. The highly contaminated area in a far distance is caused by local atmospheric precipitation which occurred between Hours 5 to 6 after the beginning of the release (the random rain intensity has uniform distribution  $U[0; 6\text{mm h}^{-1}]$ )*

## DATA ASSIMILATION – THE RIGHT WAY FROM MODEL TO REALITY

Due to complexity of the problem and uncertainties involved we can never succeed with standalone computer codes solely, even though they are as sophisticated as pos-

sible. Any pollution transport model is a simplified picture of reality. It can never comprise all features of the real world, for both theoretical and practical reasons. In its full formulation, the system of equations for the atmospheric state is of stochastic nature and describes dynamic chaos. As a consequence, the predictability of evolution of the weather conditions is limited. Solution consists in data assimilation procedures that accomplish an optimal blending of all information resources, including prior physical knowledge incorporated in the model, field observations, past experience, expert judgment and intuition.

The Bayesian approach to the estimation of the unknown quantities  $\Gamma_t$  is based on a recursive evaluation (in discrete time steps  $t$ ) of posterior probability density  $p(\Gamma_t | Y_t)$  using the Bayes rule:

Prediction step:

$$p(\Gamma_t | Y_{t-1}) = \int p(\Gamma_t | \Gamma_{t-1}) p(\Gamma_{t-1} | Y_{t-1}) d\gamma_t \quad (13a)$$

Data update step:

$$p(\Gamma_t | Y_t) \propto p(y_t | \Gamma_t) p(\Gamma_t | Y_{t-1}) \quad (13b)$$

In the prediction step the prior probability density function  $p(\Gamma_t | Y_{t-1})$  is estimated. This stands for probability of the state  $\Gamma_t$  given  $Y_{t-1}$ . The probability  $p(y_t | \Gamma_t)$  represents the *pdf* of the measurement set incoming at  $t$  given state  $\Gamma_t$ , the symbol  $\propto$  denotes equality up to a multiplicative constant. The sets of observations incoming from the same beginning in each time step of recursion up to the time interval  $t$  is arranged into the array  $Y_t = [y_1, y_2, \dots, y_t]$ .

Our contribution in this area consists in the development and application of an advanced statistical method for particle filtering (PF) based on Bayesian filtration [4]. The 3-dimensional state trajectories (particles), standing for realisations  $k, k \in \{1, \dots, K\}$  of the random system state, remain unchanged during the data (observations) update step, their weights  $w_t^k$  only being updated. Thus, the history of each path is not lost and the next time update is straightforward even when using the trajectory algorithm SGPM. The PF originating from the family of sequential Monte Carlo methods is applied here for simulation of the **posterior distribution** of the system state. During the resampling recursive procedure, partic-

les having small weights with respect to the measurements are eliminated. An arbitrary moment  $m(\Gamma_t)$  of the multidimensional *pdf* is then easily evaluated by the summation

$$m(\Gamma_t) = \sum_{k=1}^K w_t^k \cdot m(\gamma^k) \quad (14)$$

For demonstration of the PF application we adjusted the following accidental scenario. The real meteorological situation on March 31, 2009 is taken into consideration and the moment of hypothetical radioactivity release is set at 10.00 UTC. Available real meteorological observations measured near the point of the Temelin NPP and the corresponding short term meteorological forecast are somewhat inconsistent (see Table 1).

The following ex post analysis can give a retrospective view of such atypical situations (their occurrence rate is surprisingly non-negligible). The evolution of the emergency situation from the same beginning of an accident is usually so varied and complicated that specific ad hoc solutions have to be introduced. The numerical experiment described in [4] is conducted as a twin experiment where the measurements are simulated via a twin model and perturbed. Following Eq. (11), the deterministic ("best estimated") trajectory  $\gamma^{\text{best}}$  can be expressed as:

$$\gamma^{\text{best}} = \mathfrak{R} \text{SGPM}(\theta_1^{\text{best}}, \theta_2^{\text{for}}, \theta_3^{\text{for}}, \dots) \quad (15)$$

where  $\theta_1^{\text{best}}$  stands for the initially estimated value of the release source strength in the first hour and  $\theta_2^{\text{for}}, \theta_3^{\text{for}}$  are the values of wind direction and wind velocity, respectively, forecast by the ALADIN model for the first hour. From Table 1,  $\theta_1^{\text{best}} = 5.68 \times 10^{14}$  Bq,  $\theta_2^{\text{for}} = 95.0$  deg,  $\theta_3^{\text{for}} = 2.0 \text{ m.s}^{-1}$ . For the probabilistic calculations, their random nature is expressed in the standardized form  $\Theta_1 = \theta_1^{\text{best}} \cdot C_1$ ,  $\Theta_2 = \theta_2^{\text{for}} + C_2 \cdot \Delta\phi^{\text{fix}}$ ,  $\Theta_3 = \theta_3^{\text{for}} \cdot C_3$  etc. (see [4]).  $C_1, C_2$  and  $C_3$  are standardized random parameters whose distribution is determined based on expert judgement:

$$\begin{aligned} C_1 &\in \langle 0.31; 3.1 \rangle, & \text{LogUniform pdf}(c_1), \text{ median} = 1.0 \\ C_2 &\in \langle -12.0; +12.0 \rangle & \text{Uniform pdf}(c_2), \text{ median} = 0.0, \\ & & \Delta\phi^{\text{fix}} = 4.5 \text{ deg} \\ C_3 &\in \langle 0.5; 3.0 \rangle & \text{Uniform pdf}(c_3) \end{aligned} \quad (16)$$

Specifically, the "artificial" measurements in the nearest vicinity are intended for TDS on the NPP area boundary (24 positions). The remaining 54 measurement

Table 1

**A hypothetical accidental  $^{131}\text{I}$  release scenario. Short-term meteorological forecast and real meteorological measurements (in parentheses) for the Temelin NPP "point" ( $49^\circ 10' 48.53''\text{N} \times 14^\circ 22' 30.93''\text{E}$ ), time stamp 20090331-1000 UTC**

Parameter	value at UTC hour			
	10.00	11.00	12.00	13.00
$^{131}\text{I}$ activity release, Bq.h	$5.68 \times 10^{14}$	$7.92 \times 10^{14}$	0	0
wind direction <sup>1),2)</sup>	95.0 (69.0)	101.0 (65.0)	84.0 (80.0)	80.0 (64.0)
wind speed <sup>1)</sup> , $\text{m.s}^{-1}$	2.0 (3.0)	2.1 (3.3)	1.9 (3.8)	2.2 (4.0)
Pasquill atmospheric stability class	A	A	B	B

<sup>1)</sup> at 10 m height;

<sup>2)</sup> degrees measured clockwise from North



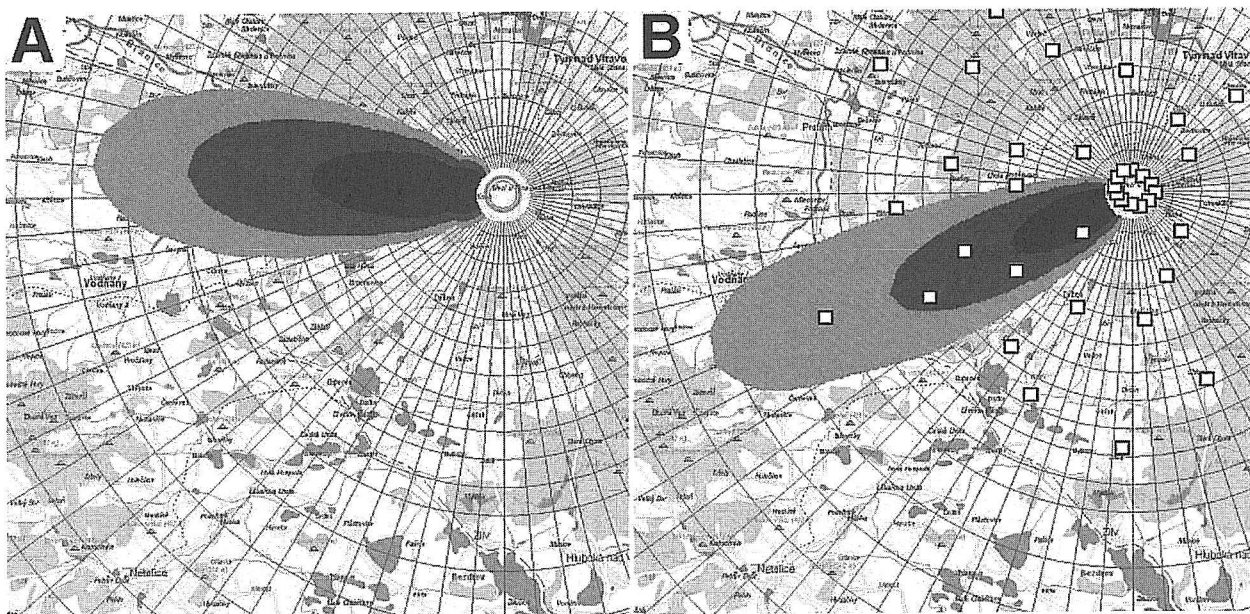


Fig. 6.  $^{131}\text{I}$  deposition obtained from the SGPM model run with the “best estimate” (nominal) model parameter values. Situation after 2 hours from the beginning of the release.

A – Meteorology according to the short term meteorological forecast (ALADIN) from Table 1;

B – Meteorology according to the real measurements (in parentheses in Table 1); release source strength decreased to one-half; White squares behind the NPP area boundary represent selected dummy measurement stations.

points (white squares in fig. 6B) are generated in positions selected deliberately so as to suit the experiment. Those “measurements” are taken from the “observation” trajectory  $\gamma^{\text{obsv}}$  calculated by the same environmental model (deterministic version of the HARP code) using real meteorological data observed near the point of the NPP (see Table 1 – values in parentheses):

$$\gamma^{\text{obsv}} = \text{sgSGPM}(\theta_1^{\text{obsv}}, \theta_2^{\text{obsv}}, \theta_3^{\text{obsv}}, \dots) \quad (17)$$

The relation  $\theta_1^{\text{obsv}} = 0.5 \cdot \theta_1^{\text{best}}$  was chosen for the subsequent demonstration of the DA capabilities (see below). The last two parameters represent the real meteorological data as included in Table 1 (data in parentheses),  $\theta_2^{\text{obsv}} = 69.0 \text{ deg}$ ,  $\theta_3^{\text{obsv}} = 3.0 \text{ m.s}^{-1}$ . The projections of the  $\gamma^{\text{best}}$  and  $\gamma^{\text{obsv}}$  trajectories into the 2-D representation of the  $^{131}\text{I}$  deposition process are illustrated in Figs. 6A and 6B, respectively.

The main results of the PF application are shown in fig. 7. The Bayesian update step assimilates the first batch of  $^{131}\text{I}$  deposition measurements (incoming in 2 hours from the beginning of the release) and enables the posterior probability density function *pdf* to be estimated. Its expectations given in fig. 7A demonstrate how to easily estimate the moments of the extremely complicated multi-dimensional state *pdf*, which is not tractable analytically. The expectation values in fig. 7A are determined from the summation equation (14) and, in fact, stand for the mean values weighted by weights resulting from the PF assimilation technique. The PF weights result from an advanced statistical treatment based on SMC modelling. A tendency of the assimilated results to lean either to model predictions (e.g. fig. 6A) or measurements (e.g. fig. 6B) is governed by mutual covariance structures of model and measurements

errors. From this point of view, the results in fig. 7A reflect our strong confidence in the accuracy of the observed field values.

Evidence of the capability of the SGPM to execute the time update step (13a) of the Bayesian recursion is given in fig. 7B. The most suitable “trajectories”, which gave rise to the results in fig. 7A, are properly proliferated and each of them is extended from the state valid for Hour 2 (fig. 7A) to the next Hour 3. The results expressed in the form of prior *pdf* expectation related to Hour 3 are illustrated in fig. 7B. Then, the Bayesian recursion can be run on the next assimilation cycle. The segmented Gaussian SGPM model provides promising results for online plume tracking and seems to be rapid enough to offer improved predictions for the impacted areas timely enough to enable appropriate decisions to be taken.

Inherent features of the PF methodology include collateral re-estimation of the actual values of major model parameters, such as the release source strength, dispersion parameters, dry deposition velocity and washing of activity from the cloud caused by atmospheric precipitation or wind field components. An example for the first three random parameters  $C_1$ ,  $C_2$  and  $C_3$  (the priors are defined by Eq. (16)) is shown in fig. 8. Knowledge from the field observations leads to a significant sharpening of the posterior histograms distributed near the selected observation values  $c_1^{\text{obsv}} = 0.5$ ,  $c_2^{\text{obsv}} = (69.0 - 95.0) / \Delta\phi^{\text{fix}} = -7.6$ . It follows from the expressions  $\theta_1^{\text{obsv}} = c_1^{\text{obsv}} \cdot \theta_1^{\text{best}}$ ,  $\theta_2^{\text{obsv}} = \theta_2^{\text{for}} + c_2^{\text{obsv}} \cdot \Delta\phi^{\text{fix}}$  and from the values in Table 1. The fuzzy results for the posterior histogram of  $C_3$  (wind velocity during the first hour of release) are related with the deficiency of observations at longer distances from the

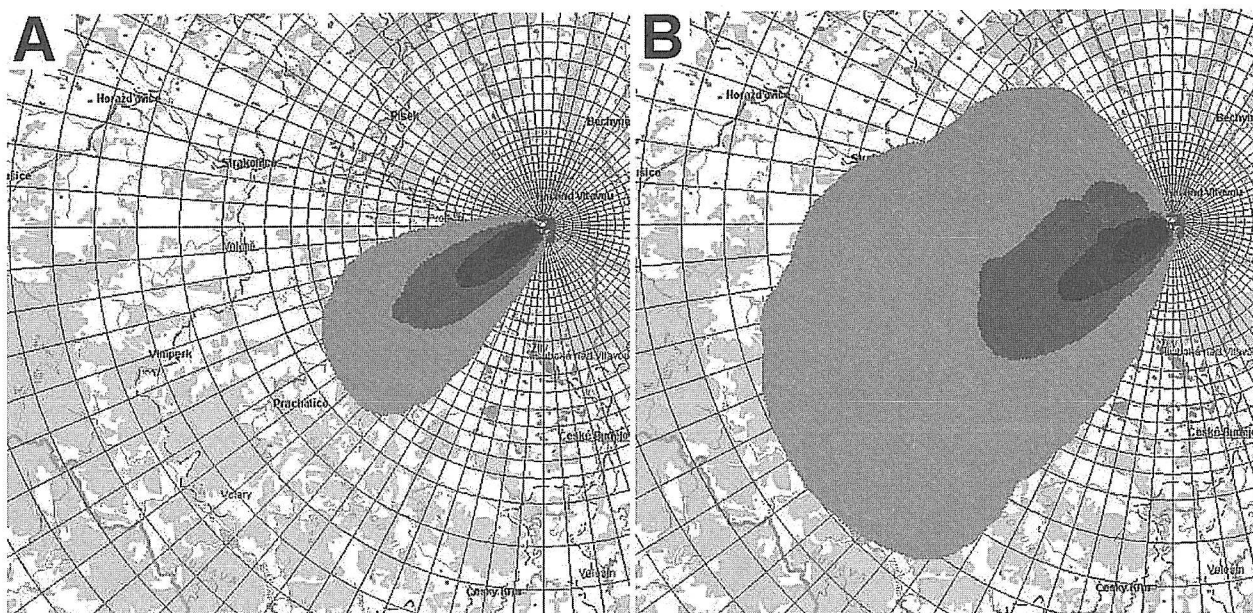


Fig. 7. *A* – Expectations of posterior pdf of the radioactivity deposition (two hours after the beginning when incoming measurements were assimilated). *B* – Prediction of the state one hour forward: prior pdf expectations for transition from Hour 2 to Hour 3.

source (see the experimental distribution of the measurement stations in fig. 6B). Thus, the originally theoretical assimilation research can provide well-founded recommendations for the spatial disposition of the measurement stations.

## SUMMARY AND CONCLUSIONS

The main features of the environmental HARP system were outlined. The system complies with the latest format of meteorological forecast and simulates dynamics of released activity. It offers an advanced interactive tool for estimation of the consequences of an accident from the initial phase of radioactivity release into the atmosphere and its further transport through the environment to humans. The rapid changes in atmospheric stability, treatment of inversion situations, transport over the complex ground and urban areas and analysis of calm situations are sources of major unresolved aspects of the advection-dispersion transport.

The fast and sufficiently accurate SGPM algorithm in combination with online connection to weather forecast and archived meteorological data make computationally intensive calculations feasible now. For instance, retrospective actual meteorological data for each hour of a year are available and accessible and enable PSA-Level3 analyses to be performed. The variability caused by meteorological changes (diurnal, seasonal etc.) can be quantified by the final statistical preprocessing. Another promising result has been achieved in the assessment of long-term radiological consequences of normal NPP operation. The practicability of the HARP code for future EIA studies has been confirmed.

Probabilistic modelling of uncertainty propagation through the model provides an adequate basis for uncer-

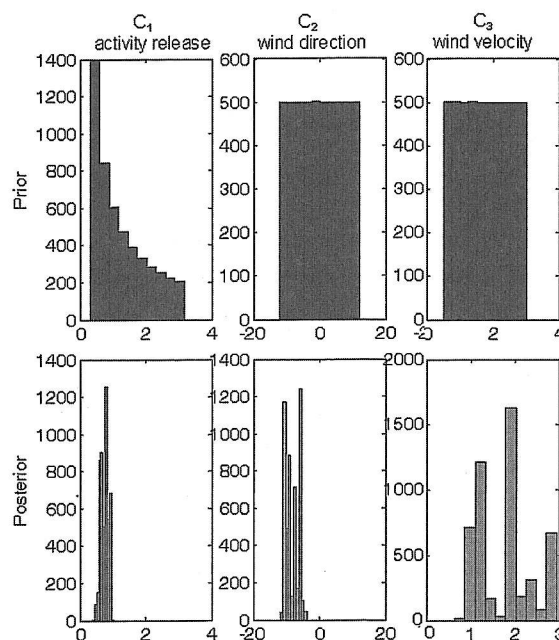


Fig. 8. Comparison between the prior (top row) and posterior (bottom row) histograms of distribution of selected random parameters  $C_1$ ,  $C_2$ ,  $C_3$  (see definition in equation (16))

tainty and sensitivity analysis and introduction of advanced consequence assessment procedures. It makes it possible to apply recent trends in the risk assessment methodology, consisting in a transition from deterministic procedures to the probabilistic approach which enables more informative probabilistic answers on assessment questions to be generated.

The most important achievements include the development of special data assimilation techniques and their application in the early and late stages of a radiation acci-

dent. The adopted procedure of the Particle Filter seems to be robust enough and suitable to manage some discrepancies and scenario incompleteness occurring from the beginning of the accident. Nesting of the data assimilation cycles within the predictions in the particular time steps seems to be crucial for an improvement of emergency preparedness provisions.

In the field of data assimilation progressions, many questions remain to be answered. Important problems relate to the availability and accessibility of measurements and require establishing a dialogue and cooperation with radiation monitoring network data providers. An attention should be focused on incorporation of indirect measurements, intermittent or continuous mode of incoming observations, more precise elaboration of covariance structure of measurement errors, coverage density of measurements stations etc.

#### Acknowledgement

This work was supported by the Czech Grant Agency, grant project No. 02/07/1596. The authors thank to colleagues from the MEDARD working group at the Institute of Computer Science, Academy of Sciences of the Czech Republic, for their help with the MM5 gridded meteorological data format during the tests of potential utilisation of knowledge from the Lagrangian HYSPLIT model.

#### Acronyms and symbols

ADM	Atmospheric Dispersion Model
ALADIN	model of numerical weather forecast on a limited 3-D area
CET	Central European Time
DA	Data Assimilation
DEP	DEPosited radioactivity on the ground
EIA	Environmental Impact Assessment
FCM	Food Chain Model
$\Gamma_t$	random state vector
HARP	Hazardous Radioactivity Propagation program system
K	for SGPM shifts: number of elemental shifts; for uncertainty analysis: number of stratified samples of vector of model parameters
LHS	Latin Hypercube Sampling scheme
M	number of input model parameters regarded as random in the HARP code
MM5	Numerical weather Mesoscale Model of 5 <sup>th</sup> generation
N	dimension of background vector (number of polar nodes of computational grid)
NPP	Nuclear Power Plant
<i>pdf</i>	probability density function
$p(y_t   \Gamma_t)$	conditional <i>pdf</i> of measurement set $y_t$ at $t$ given state $\Gamma_t$
PF	assimilation technique of Bayesian Particle Filtering
PSA	Probabilistic Safety Assessment

RDD	Radiological Dispersion Device
SGPM	Segmented Gaussian Plume Model
SMC	Sequential Monte Carlo methods
TDS	TeleDosimetric System
TIC	Time Integral of near-ground specific activity Concentration in air
UA, SA	Uncertainty Analysis, Sensitivity Analysis
UTC	Universal Time Coordinated

#### References

- [1] DOUCET, A., DE FREITAS, N., GORDON, N. J. (eds.): Sequential Monte Carlo method in practice. Springer-Verlag, New York, 2001.
- [2] DRAXLER, R. R., HESS, G. D.: Description of the HYSPLIT\_4 Modelling System. NOAA Tech. Memorandum, ERL ARL-224, rev. 2004.
- [3] KUČA, P., HOFMAN, R., PECHA, P.: Assimilation techniques in consequence assessment of accidental radioactivity releases – the way for increase of reliability of predictions. In Proc. of ECORAD 2008, Bergen, Norway, June 15-20, 2008, 138-141.
- [4] PECHA, P., HOFMAN, R., ŠMÍDL, V.: Bayesian tracking of the toxic plume spreading in the early stage of radiation accident. In Proc. of European Simul. and Modelling Conference ESM'2009, Leicester, UK, Oct. 26-28, 2009, pp. 381-387.
- [5] PECHA, P., PECHOVÁ E., KELEMEN R.: Application of system HAVAR-RP in the field of radiation protection. HAVAR-RP archive, 2006, rev. 2009. In the Czech.
- [6] PECHA, P., HOFMAN, R.: HARP – A Software Tool for Decision Support during Nuclear Emergencies. TIES 2009 – The 20th Annual Conference of International Environmetrics Society, Handling Complexity and Uncertainty in Environmental Studies, (Bologna, IT, July 5-7, 2009).
- [7] PECHA, P., HOFMAN, R., PECHOVÁ E.: Training simulator for analysis of environmental consequences of accidental radioactivity releases. In Proc. of the 6th EUROSIM Congress on Modelling and Simulation, Eds: Zupančič Borut, Ljubljana, SI, Sept. 9 – 13, 2007.
- [8] HOFMAN, R., PECHA, P., PECHOVÁ E.: A Simplified Approach for Solution of Time Update Problem during Toxic Waste Plume Spreading in the Atmosphere. In Proc. of HARMO12-12<sup>th</sup> Inter. Conf. on Harmonization within Atmospheric Dispersion Modelling for Regulatory Purposes, Hrvatski Meteorološki Časopis, Paper No. H12-57, pp. 510-515, Cavtat, HR, Oct. 6 -10, 2008.
- [9] KUČA, P., PECHA, P., HOFMAN, R.: Lessons learned from former radiation accidents on development of software tools for effective decision making support. In Proc. of 11<sup>th</sup> In. Conf. on Present and Future of Crisis Management. Praha, CZ, Nov. 23 – 24, 2009, ISBN 978-80-254-5913-3.

Recenzoval: Z. Prouza